Biophysical Journal
Article

Biophysical Society

Molecular Mechanisms of the R61T Mutation in Apolipoprotein E4: A Dynamic Rescue

Benfeard Williams II,[1] Marino Convertino,[1] Jhuma Das,[1] and Nikolay V. Dokholyan[1,*]
[1]Biochemistry and Biophysics Department, University of North Carolina, Chapel Hill, North Carolina

ABSTRACT The apolipoprotein E4 (ApoE4) gene is the strongest genetic risk factor for Alzheimer's disease (AD). With respect to the other common isoforms of this protein (ApoE2 and ApoE3), ApoE4 is characterized by lower stability that underlies the formation of a stable interaction between the protein's N- and C-terminal domains. AD-related cellular dysfunctions have been linked to this ApoE4 misfolded state. In this regard, it has been reported that the mutation R61T is able to rescue the deleterious cellular effects of ApoE4 by preventing the formation of the misfolded intermediate state. However, a clear description of the structural features at the basis of the R61T-ApoE4 mutant's protective effect is still missing. Recently, using extensive molecular dynamics simulations, we have identified a structural model of an ApoE4 misfolded intermediate state. Building on our previous work, here we explore the dynamical changes induced by the R61T mutation in the ApoE4 native and misfolded states. Notably, we do not observe any local changes in the domains in the R61T-ApoE4 system, rather a general loss of correlated movements in the entire protein structure. More specifically, we detect increased dynamics in the hinge region, which is essential for ApoE4 domain-domain interaction. Consistent with previously reported data on altered phospholipid and receptor binding, we hypothesize that mutations destabilizing the ApoE4 intermediate state change hinge region dynamics, which propagates to distal functional regions of the protein and modifies ApoE4's functional properties. This unique behavior of the ApoE4 hinge region provides, to our knowledge, a novel understanding of ApoE4's role in AD.

INTRODUCTION

The E4 isoform of Apolipoprotein E (ApoE4) is the strongest genetic risk factor for Alzheimer's disease (AD) and it is found in 80% of familial and 64% of sporadic cases of AD (1). ApoE4 is a 299-residue lipid binding protein, expressed in the highest concentrations in the liver and the brain (2,3). Three common ApoE isoforms are known and they differ by a single amino acid, with ApoE3 isoform being the most common (~75% of the population) and neutral toward the risk of AD onset, and ApoE2 known to be protective against AD (~10% of the population) (1,4–6). Structurally, all ApoE isoforms are similar, consisting of a four-helix bundle N-terminal domain and an elongated C-terminal domain linked by a hinge region (Fig. S1 *A*), but only ApoE4 is implicated in the onset of AD. The role of ApoE4 in the development of AD is poorly understood. It has been shown that ApoE4 has multiple implications in AD pathology such as altered amyloid beta (Aβ) clearance, mitochondria function, cholesterol efflux, and posttranslational modification of tau protein (5,7–14). Additionally, ApoE4 is the least thermally stable ApoE isoform, leading to a folded intermediate state, characterized as a molten globule (15). We have previously derived the structural model of the ApoE4 stable misfolded intermediate (Fig. S1 *B*) (16), which may explain the pathological behavior of ApoE4 in AD. Indeed, a defining characteristic of the ApoE4 intermediate conformation is the interdomain interaction involving the N- and C-terminal domains of the protein. It has been hypothesized that the interdomain interaction in ApoE4 may be mediated by a salt-bridge interaction involving residues R61 and E255 (17). However, alternative hypotheses exist that do not align with the presence of an R61-E255 salt bridge (16,18,19). Moreover, data in the literature report that mutation of R61 to threonine abolishes the intermediate state and pathological effects on cells in vitro (20,21). It has also been observed in Aβ peptide processing studies that ApoE4 increases Aβ production relative to ApoE3 (7). When introducing the R61T mutation to ApoE4 in cells, the increase in Aβ production is attenuated (7). The R61T mutation also rescues cells from detrimental effects such as reduced mitochondrial motility and reduced neurite outgrowth (21). Additionally, R61T improves intracellular trafficking in the endoplasmic reticulum and Golgi apparatus (22). Previous studies of mice ApoE4,

Submitted May 15, 2017, and accepted for publication August 17, 2017.
*Correspondence: dokh@unc.edu
Editor: Nathan Baker.
http://dx.doi.org/10.1016/j.bpj.2017.08.026

which contains T61 at the equivalent position in the wild-type sequence and exhibits no domain-domain interaction, indicate that the protective effect of the R61T mutation stems from its destabilization of the ApoE4 misfolded intermediate state (23). Additionally, T61R in mice changes the preference of ApoE4 binding from high density lipoprotein to very low density lipoprotein, mirroring the change in preference exhibited by R61T in humans from very low density lipoprotein to high density lipoprotein (24). Here we explore the impact of the R61T mutation on the ApoE4 structure at molecular level to understand the changes elicited by the mutation. Our goal is to elucidate the specific structural features that underlie the rescuing behavior of the R61T mutation in correcting the physiological functions of ApoE4. We observe changes in the dynamics and end-to-end distance of the hinge region (d_{hinge}) in the previously identified ApoE4 misfolded intermediate state conformation. Specifically, correlations between the N- and C-terminal domains with the hinge region are strengthened. This enhanced long-range communication can potentially facilitate the inhibition of domain-domain interaction and interfere with both the harmful effects leading to the onset of AD as well as changes in lipid binding activity by destabilizing ApoE4 intermediate structures.

MATERIALS AND METHODS

We generate a native state model of ApoE4 starting from the 3D coordinates of ApoE3 (18) obtained by NMR as described by Williams et al. (16). The structural model of the ApoE4 misfolded intermediate state is derived from a clustering analysis of replica exchange discrete molecular dynamics (DMD) simulations performed as previously described (16). We implement the protein design suite, *Eris*, on both the native and intermediate state models to generate R61T mutant structures (25,26). Additionally, our *Eris* calculations evaluate the relative thermodynamic stability of protein structures upon mutation by calculating $\Delta\Delta G$ values. $\Delta\Delta G$ is quantified as the change in free energy based on the difference between the wild-type and mutant protein systems (25,26). The free energy is expressed as a weighted sum of van der Waals forces, solvation, hydrogen bonding, and backbone-dependent statistical energies. For all generated ApoE4 systems, we perform five, independent, 2×10^6 time step (~100 ns) DMD simulations at a temperature of 0.4 kcal/(mol k_B) (T = ~200 K) (27–30). Indeed, such a low temperature minimizes the effect of thermal fluctuations when evaluating the intrinsic differences between the wild-type (WT) and mutant sequences of ApoE4. A thorough analysis of the systems under investigation is performed using the software Wordom (31,32). We report atomic distances, radius of gyration (Rg), root mean square deviation (RMSD), and root mean square fluctuations of Cα atoms computed over five independent simulations. Secondary structure calculations are performed using the DSSP algorithm. We exclude the first 5×10^5 time steps (~25 ns) required for system equilibration based on the RMSD and potential energy of both systems (Fig. S2). We further calculate the dynamic cross-correlation (DCC) coefficients among ApoE4 Cα atoms. We quantify the DCC coefficient Cij as follows:

$$C_{ij} = \frac{\overline{\left(r_i - \overline{r_i}\right)\left(r_j - \overline{r_j}\right)}}{\sqrt{\left(r_i^2 - \overline{r_i^2}\right)\left(r_j^2 - \overline{r_j^2}\right)}}, \quad (1)$$

where r_i and r_j are the corresponding position vectors of Cα atoms i and j. We consider only the top 1% interactions among all the correlations, C_{ij}. Additionally, we filter out all correlation between residue i and residue $j <= i + 5$ to remove the strong positive correlations along α-, 3_{10}-, and π-helices. Circle plots displaying the DCC coefficients for each ApoE isoform are generated using ad hoc PYTHON scripts (https://www.python.org) where the corresponding ApoE4 sequence is displayed clockwise along the perimeter of the circle (Figs. 3 and 4).

RESULTS AND DISCUSSION

To investigate how R61T affects the structure of the ApoE4 native and misfolded intermediate states, we calculate the RMSD distributions along the entire DMD simulations of both WT- and R61T-ApoE4 systems (Fig. 1). No relevant differences in the RMSD distributions are observed. For all of the systems under investigation, the explored RMSD range is <2 Å, which corresponds with the negligible changes in the overall topology of the systems as confirmed by visual inspection. Consistently, we observe only minor changes in the Rg of the all analyzed systems (Fig. 2 *A*). Despite a minimal variation in the volume of the WT- and R61T-ApoE4 structures, we observe that Rg is decreasing for ApoE4 native state and increasing in the misfolded intermediate state with the R61T mutation. Such behavior is consistent throughout the entire set of simulations and can be attributed to the difference in amino acid side-chain packing that affects the protein volume. However, a visual inspection of the simulations reveals that peaks in RMSD distributions can be attributed to an accordion-like movement of ApoE4 N- and C-terminal domains (Fig. S3). This observation leads us to focus on the long-range effects of R61T on the dynamics of the hinge region, which connects the two protein domains.

The hinge region plays a critical role in mediating the formation of the interdomain interactions that characterizes the ApoE4 intermediate state (33). To address changes that may

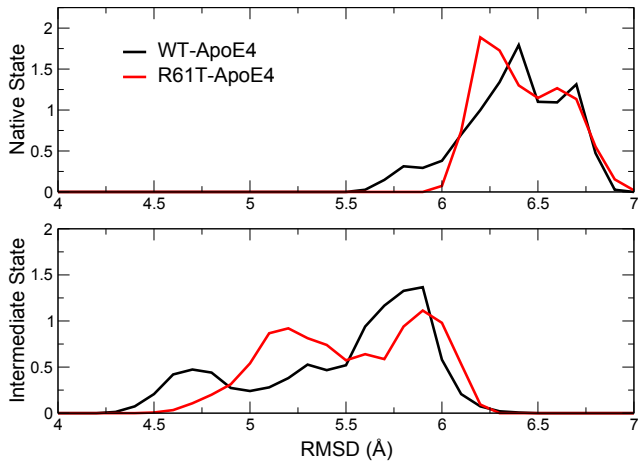

FIGURE 1 RMSD distributions for WT- and R61T-ApoE4 systems. To see this figure in color, go online.

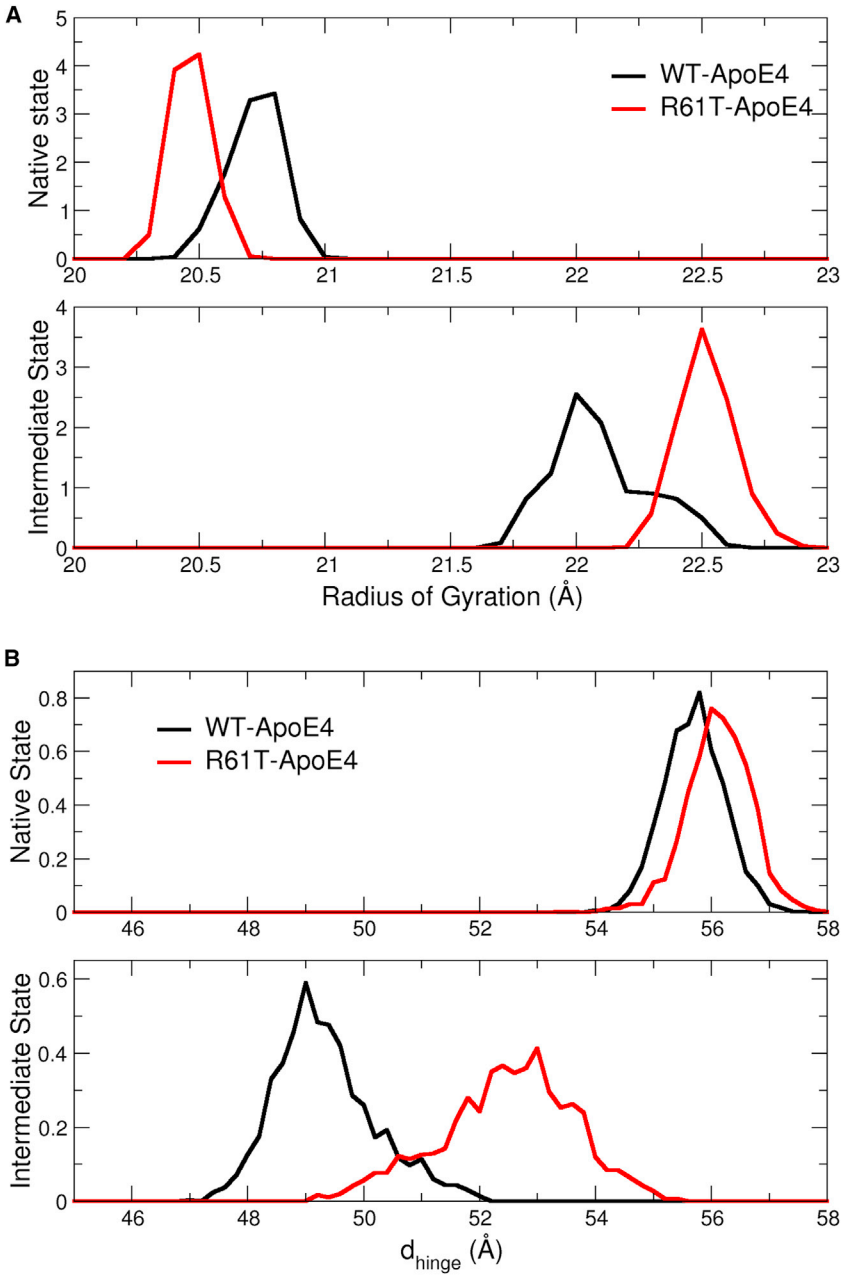

FIGURE 2 Distributions of the (*A*) radius of gyration (*Rg*) and (*B*) end-to-end distance of the hinge region (d_{hinge}) for wild-type and R61T-ApoE4 systems. *t*-test values are 3.6×10^{-14} and 4.2×10^{-80} for 100 random data points from the native and intermediate states distributions, respectively. To see this figure in color, go online.

occur at this location due to the destabilizing mutation R61T as predicted by our Eris calculations ($\Delta\Delta G_{\text{Native}}$ 3.71 ± 0.69 kcal/mol; $\Delta\Delta G_{\text{Intermediate}} = 3.11 \pm 0.44$ kcal/mol), we measure the Euclidean distance between Cα atoms of residues 166 and 206 that constitute the two extremities of the hinge region, d_{hinge} (Fig. 2 *B*). Whereas there is no significant change in d_{hinge} for the native state, the overall d_{hinge} is greater in the R61T-ApoE4 intermediate state. This particular behavior can be related to the disruption of the intermediate state. Indeed, it has been shown that the R61T mutation in ApoE4 disrupts interdomain interaction through C-terminal domain destabilization, which can be propagated via the hinge region (20,34). Additionally, NMR studies and our simulations reveal that the hinge can extend specifically in the ApoE4 isoform (35). This underestimated role of the hinge region in mediating the pathological formation of the

TABLE 1 Secondary Structure Content of ApoE4 Hinge Region for WT- and R61T-ApoE4 Systems

	Secondary Structure	WT (%)	R61T (%)
Native state	α-helical	36.7 ± 6.3	40.0 ± 10.0
	disordered	41.9 ± 7.4	44.0 ± 7.6
	β-strand	4.2 ± 3.2	4.5 ± 4.7
Intermediate state	α-helical	39.3 ± 5.9	41.5 ± 6.3
	disordered	46.3 ± 7.5	46.1 ± 7.9
	β-strand	6.9 ± 4.9	3.8 ± 3.2

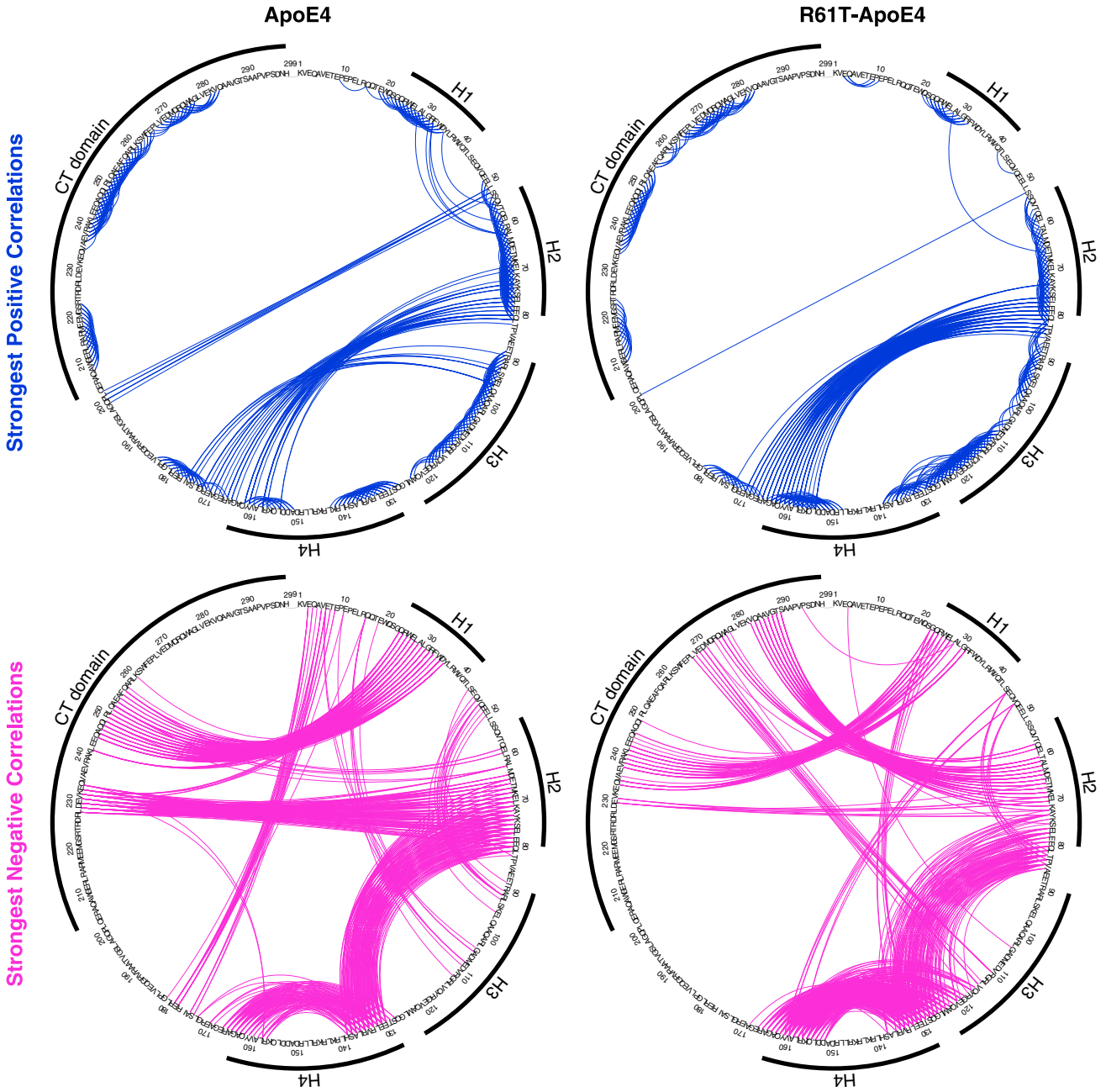

FIGURE 3 Dynamic cross-correlation coefficients among ApoE4 residues in the native state conformation. Dynamic cross-correlation coefficients are plotted as lines on circle plots. The sequence of the WT- and R61T-ApoE4 systems circles the perimeter in a clockwise direction. The strongest positive and negative correlations are represented in the upper and lower circle plots, respectively (see Materials and Methods). Secondary structure elements, helices 1–4 (H1–H4), and the C-terminal (*CT*) domain, are indicated with bars around the perimeter. The distribution of coefficients trend toward more positive correlations in the R61T-ApoE4 system relative to WT-ApoE4 (*t*-test value of 5.1×10^{-11}). To see this figure in color, go online.

intermediate state is consistent with the data reported in the literature (17,33,36).

We further investigate the secondary structure of the hinge region to determine if the changes in d_{hinge} were due to changes in hydrogen bonding. The helical content of the hinge region remains the same in both the native and intermediate states after introducing the R61T mutation (Table 1). This reinforces that the changes induced by the R61T mutation affect the overall positioning of the hinge region between the N- and C-terminal domains rather than the structural topology. The R61T mutations maintain the highly disordered structure of this domain-linking region (Fig. S1).

To further investigate R61T-induced changes within the hinge region and the rest of the ApoE4, we analyze DCC coefficients among all protein residues. Specifically, we focus

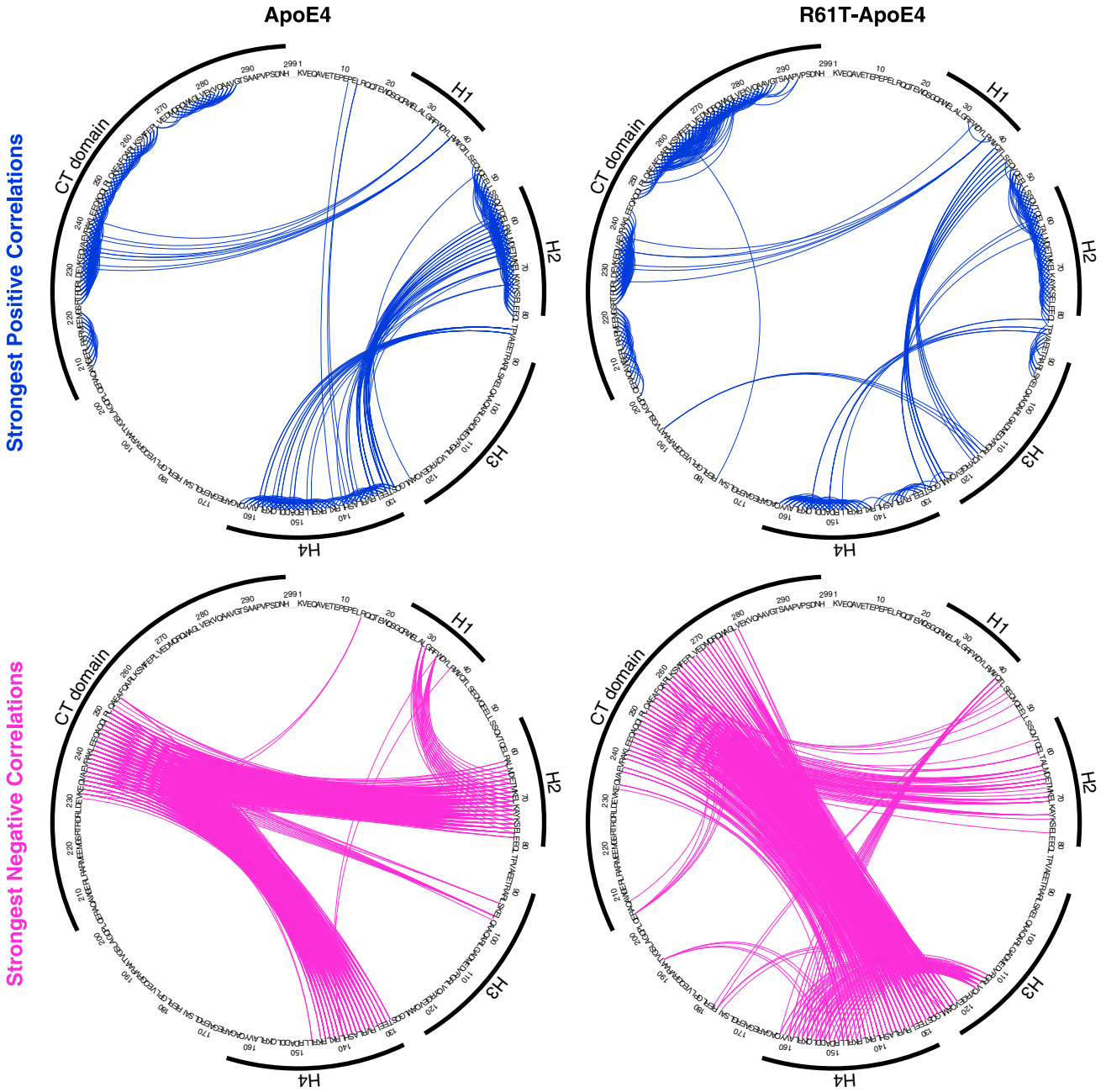

FIGURE 4 Dynamic cross-correlation coefficients among ApoE4 residues in the intermediate state conformation. Dynamic cross-correlation coefficients are plotted as lines on circle plots. The sequence of the WT- and R61T-ApoE4 systems circles the perimeter in a clockwise direction. The strongest positive and negative correlations are represented in the upper and lower circle plots, respectively (see Materials and Methods). Secondary structure elements, helices 1–4 (H1–H4) and the C-terminal (*CT*) domain, are indicated with bars around the perimeter. The WT- and ApoE4 systems have a similar distribution of coefficient values (*t*-test value of 0.3). To see this figure in color, go online.

on the strongest (both positive and negative) correlations for both WT- and R61T-ApoE4 systems. In the ApoE4 native state conformation, we observe similar strong positive correlation for WT- and R61T-ApoE4 systems. The R61T mutation weakens correlations between helix 1 (H1) and helix 2 (H2), as well as the correlations between helix 3 (H3) and the hinge region (Fig. 3). R61T also induces a severe weakening of strong negative correlations involving the hinge region (Fig. 3). These changes and rearrangements in both the positive and negative DCC coefficients are consistent with our stability calculations using Eris (25,26) and our DMD simulations suggesting that R61T may destabilize the ApoE4 native state (Fig. S4). Additionally, with the R61T mutation, the weakening of correlations involving the hinge region, as well as the ones between the N- and C-terminal domains, may be indicative of the

inability to form domain-domain interactions (20). These alterations, particularly in the C-terminal domain, which contains the lipid binding region, are consistent with the reported changes in lipoprotein binding preference as a consequence of the R61T mutation (36).

We also analyze DCC coefficients for our structural model of the ApoE4 misfolded intermediate state. Upon introduction of the R61T mutation, both positive and negative correlations involving the hinge region are strengthened, whereas negative correlations involving the N- and C-terminal domains become more dispersed across a greater number of residues (Fig. 4). These changes in the hinge region support our previous findings that R61T is directly affecting the hinge region conformational space (Fig. 2 *B*). We propose that the modifications in the dynamics of the hinge region lead to the change in correlations observed between the N- and C-terminal domains. These altered hinge dynamics may explain the prevention of domain-domain interaction in the R61T-ApoE4 system.

Building on the results of our DMD simulations of the R61T-ApoE4, we hypothesize that the mode of action for this mutation is to alter long-range communication within the protein, which abolishes its interdomain interaction (20). This hypothesis is consistent with allosteric effects generated in ApoE4 by mutations at the position 61 (19,37). This phenomenon remains unique to ApoE4 as our DCC studies with ApoE2 and ApoE3 present changes only within the N-terminal domain (data not shown). Additionally, functional studies have shown that cells expressing ApoE4 secrete fewer phospholipids than ApoE3-expressing cells (20), whereas ApoE3-matching phospholipid concentrations are observed in cells expressing R61T-ApoE4 (20). This finding suggests that beyond domain-domain interaction, the altered dynamics in the hinge region may be responsible for altering ApoE4 phospholipid-binding capacity. Indeed, it is known that lipid levels (i.e., phospholipid, cholesterol) also affects amyloid precursor peptide processing, which could be altered by hinge region dynamics and correlations with the C-terminal domain, which contains the lipid binding motif (38,39). Considering the importance of the hinge region for domain-domain interaction (33), we believe that changes in its dynamics might be responsible for the ApoE4-mediated onset of AD.

CONCLUSION

We propose that destabilizing mutations on the ApoE4 may not affect the folding of the native state, but, rather, alter the dynamics of the N- and C-terminal domains via the hinge region. These changes in ApoE4 dynamics (relative to the other two common ApoE isoforms), may be responsible for both altered lipid metabolism and onset of AD. Our results suggest that the hinge region is more than a domain linker that has merely been suggested as a site of potential proteolytic cleavage (10,38,40–44). Our findings point to a pivotal role of the hinge region in ApoE4, designating it a unique target for abolishing the detrimental events associated with the ApoE4 isoform because the hinge region has a significant allosteric effect on the N- and C-terminal domains. Starting from our observations and hypotheses, we invite the scientific community to take advantage of this, to our knowledge, new information as an alternative and unexplored avenue for experimentally studying the role of ApoE4 in AD.

SUPPORTING MATERIAL

Four figures are available at http://www.biophysj.org/biophysj/supplemental/S0006-3495(17)30919-0.

AUTHOR CONTRIBUTIONS

B.W., M.C., J.D., and N.V.D. designed the experiments. B.W. performed the molecular dynamics simulations. B.W., M.C., J.D., and N.V.D. analyzed the data and wrote the manuscript.

ACKNOWLEDGMENTS

This work is supported by National Institutes of Health (NIH) grants R01GM080742, R01GM11401, R01GM064803, and R01GM123247 to N.V.D.

REFERENCES

1. Corder, E. H., A. M. Saunders, …, M. A. Pericak-Vance. 1993. Gene dose of apolipoprotein E type 4 allele and the risk of Alzheimer's disease in late onset families. *Science.* 261:921–923.
2. Mahley, R. W. 1988. Apolipoprotein E: cholesterol transport protein with expanding role in cell biology. *Science.* 240:622–630.
3. Weisgraber, K. H. 1994. Apolipoprotein E: structure-function relationships. *Adv. Protein Chem.* 45:249–302.
4. Corder, E. H., A. M. Saunders, …, M. A. Pericak-Vance. 1994. Protective effect of apolipoprotein E type 2 allele for late onset Alzheimer disease. *Nat. Genet.* 7:180–184.
5. Mahley, R. W., K. H. Weisgraber, and Y. Huang. 2006. Apolipoprotein E4: a causative factor and therapeutic target in neuropathology, including Alzheimer's disease 103:5644–5651.
6. Hauser, P. S., and R. O. Ryan. 2013. Impact of apolipoprotein E on Alzheimer's disease. *Curr. Alzheimer Res.* 10:809–817.
7. Ye, S., Y. Huang, …, R. W. Mahley. 2005. Apolipoprotein (Apo) E4 enhances amyloid β peptide production in cultured neuronal cells: apoE structure as a potential therapeutic target. *Proc. Natl. Acad. Sci. USA.* 102:18700–18705.
8. Holtzman, D. M., K. R. Bales, …, S. M. Paul. 2000. Apolipoprotein E isoform-dependent amyloid deposition and neuritic degeneration in a mouse model of Alzheimer's disease. *Proc. Natl. Acad. Sci. USA.* 97:2892–2897.
9. Garai, K., P. B. Verghese, …, C. Frieden. 2014. The binding of apolipoprotein E to oligomers and fibrils of amyloid-β alters the kinetics of amyloid aggregation. *Biochemistry.* 53:6323–6331.
10. Brecht, W. J., F. M. Harris, …, Y. Huang. 2004. Neuron-specific apolipoprotein e4 proteolysis is associated with increased tau phosphorylation in brains of transgenic mice. *J. Neurosci.* 24:2527–2534.

11. Tesseur, I., J. van Dorpe, …, F. Van Leuven. 2000. Expression of human apolipoprotein E4 in neurons causes hyperphosphorylation of protein tau in the brains of transgenic mice. *Am. J. Pathol.* 156:951–964.
12. Harris, F. M., W. J. Brecht, …, Y. Huang. 2004. Increased tau phosphorylation in apolipoprotein E4 transgenic mice is associated with activation of extracellular signal-regulated kinase: modulation by zinc. *J. Biol. Chem.* 279:44795–44801.
13. Strittmatter, W. J., A. M. Saunders, …, A. D. Roses. 1994. Isoform-specific interactions of apolipoprotein E with microtubule-associated protein tau: implications for Alzheimer disease. *Proc. Natl. Acad. Sci. USA.* 91:11183–11186.
14. Mahley, R. W. 2016. Apolipoprotein E: from cardiovascular disease to neurodegenerative disorders. *J. Mol. Med. (Berl.).* 94:739–746.
15. Morrow, J. A., D. M. Hatters, …, K. H. Weisgraber. 2002. Apolipoprotein E4 forms a molten globule. A potential basis for its association with disease. *J. Biol. Chem.* 277:50380–50385.
16. Williams, B., 2nd, M. Convertino, …, N. V. Dokholyan. 2015. ApoE4-specific misfolded intermediate identified by molecular dynamics simulations. *PLOS Comput. Biol.* 11:e1004359.
17. Dong, L. M., and K. H. Weisgraber. 1996. Human apolipoprotein E4 domain interaction. Arginine 61 and glutamic acid 255 interact to direct the preference for very low density lipoproteins. *J. Biol. Chem.* 271:19053–19057.
18. Chen, J., Q. Li, and J. Wang. 2011. Topology of human apolipoprotein E3 uniquely regulates its diverse biological functions. *Proc. Natl. Acad. Sci. USA.* 108:14813–14818.
19. Frieden, C., and K. Garai. 2013. Concerning the structure of apoE. *Protein Sci.* 22:1820–1825.
20. Xu, Q., W. J. Brecht, …, Y. Huang. 2004. Apolipoprotein E4 domain interaction occurs in living neuronal cells as determined by fluorescence resonance energy transfer. *J. Biol. Chem.* 279:25511–25516.
21. Chen, H.-K., Z. Liu, …, R. W. Mahley. 2012. Small molecule structure correctors abolish detrimental effects of apolipoprotein E4 in cultured neurons. *J. Biol. Chem.* 287:5253–5266.
22. Brodbeck, J., J. McGuire, …, Y. Huang. 2011. Structure-dependent impairment of intracellular apolipoprotein E4 trafficking and its detrimental effects are rescued by small-molecule structure correctors. *J. Biol. Chem.* 286:17217–17226.
23. Zhong, N., G. Ramaswamy, and K. H. Weisgraber. 2009. Apolipoprotein E4 domain interaction induces endoplasmic reticulum stress and impairs astrocyte function. *J. Biol. Chem.* 284:27273–27280.
24. Raffai, R. L., L. M. Dong, …, K. H. Weisgraber. 2001. Introduction of human apolipoprotein E4 "domain interaction" into mouse apolipoprotein E. *Proc. Natl. Acad. Sci. USA.* 98:11587–11591.
25. Yin, S., F. Ding, and N. V. Dokholyan. 2007. Eris: an automated estimator of protein stability. *Nat. Methods.* 4:466–467.
26. Yin, S., F. Ding, and N. V. Dokholyan. 2007. Modeling backbone flexibility improves protein stability estimation. *Structure.* 15:1567–1576.
27. Dokholyan, N. V., S. V. Buldyrev, …, E. I. Shakhnovich. 1998. Discrete molecular dynamics studies of the folding of a protein-like model. *Fold. Des.* 3:577–587.
28. Ding, F., D. Tsao, …, N. V. Dokholyan. 2008. Ab initio folding of proteins with all-atom discrete molecular dynamics. *Structure.* 16:1010–1018.
29. Proctor, E. A., F. Ding, and N. V. Dokholyan. 2011. Discrete molecular dynamics. *WIREs Comput. Mol. Sci.* 1:80–92.
30. Shirvanyants, D., F. Ding, …, N. V. Dokholyan. 2012. Discrete molecular dynamics: an efficient and versatile simulation method for fine protein characterization. *J. Phys. Chem. B.* 116:8375–8382.
31. Seeber, M., M. Cecchini, …, A. Caflisch. 2007. Wordom: a program for efficient analysis of molecular dynamics simulations. *Bioinformatics.* 23:2625–2627.
32. Seeber, M., A. Felline, …, F. Fanelli. 2011. Wordom: a user-friendly program for the analysis of molecular structures, trajectories, and free energy surfaces. *J. Comput. Chem.* 32:1183–1194.
33. Zhang, Y., S. Vasudevan, …, J. Wang. 2007. A monomeric, biologically active, full-length human apolipoprotein E. *Biochemistry.* 46:10722–10732.
34. Nguyen, D., P. Dhanasekaran, …, S. Lund-Katz. 2014. Influence of domain stability on the properties of human apolipoprotein E3 and E4 and mouse apolipoprotein E. *Biochemistry.* 53:4025–4033.
35. Chetty, P. S., L. Mayne, …, M. C. Phillips. 2017. Helical structure, stability, and dynamics in human apolipoprotein E3 and E4 by hydrogen exchange and mass spectrometry. *Proc. Natl. Acad. Sci. USA.* 114:968–973.
36. Dong, L. M., C. Wilson, …, D. A. Agard. 1994. Human apolipoprotein E. Role of arginine 61 in mediating the lipoprotein preferences of the E3 and E4 isoforms. *J. Biol. Chem.* 269:22358–22365.
37. Frieden, C., and K. Garai. 2012. Structural differences between apoE3 and apoE4 may be useful in developing therapeutic agents for Alzheimer's disease. *Proc. Natl. Acad. Sci. USA.* 109:8913–8918.
38. Bodovitz, S., and W. L. Klein. 1996. Cholesterol modulates α-secretase cleavage of amyloid precursor protein. *J. Biol. Chem.* 271:4436–4440.
39. Fassbender, K., M. Simons, …, T. Hartmann. 2001. Simvastatin strongly reduces levels of Alzheimer's disease β-amyloid peptides Aβ 42 and Aβ 40 in vitro and in vivo. *Proc. Natl. Acad. Sci. USA.* 98:5856–5861.
40. Marques, M. A., M. Tolar, …, K. A. Crutcher. 1996. A thrombin cleavage fragment of apolipoprotein E exhibits isoform-specific neurotoxicity. *Neuroreport.* 7:2529–2532.
41. Harris, F. M., W. J. Brecht, …, Y. Huang. 2003. Carboxyl-terminal-truncated apolipoprotein E4 causes Alzheimer's disease-like neurodegeneration and behavioral deficits in transgenic mice. *Proc. Natl. Acad. Sci. USA.* 100:10966–10971.
42. Wellnitz, S., A. Friedlein, …, C. Czech. 2005. A 13 kDa carboxy-terminal fragment of ApoE stabilizes Aβ hexamers. *J. Neurochem.* 94:1351–1360.
43. Rohn, T. T. 2013. Proteolytic cleavage of apolipoprotein E4 as the keystone for the heightened risk associated with Alzheimer's disease. *Int. J. Mol. Sci.* 14:14908–14922.
44. Tamboli, I. Y., D. Heo, and G. W. Rebeck. 2014. Extracellular proteolysis of apolipoprotein E (apoE) by secreted serine neuronal protease. *PLoS One.* 9:e93120.